Originally posted 23 August 2012; corrected 16 October 2012

www.sciencemag.org/cgi/content/full/science.1226344/DC1

Supplementary Materials for

Genome Sequencing Identifies a Basis for Everolimus Sensitivity

Gopa Iyer, Aphrothiti J. Hanrahan, Matthew I. Milowsky, Hikmat Al-Ahmadie, Sasinya N. Scott, Manickam Janakiraman, Mono Pirun, Chris Sander, Nicholas D. Socci, Irina Ostrovnaya, Agnes Viale, Adriana Heguy, Luke Peng, Timothy A. Chan, Bernard Bochner, Dean F. Bajorin, Michael F. Berger, Barry S. Taylor,* David B. Solit*

*To whom correspondence should be addressed. E-mail: barry.taylor@ucsf.edu (B.S.T.); solitd@mskcc.org (D.B.S.)

Published 23 August 2012 on *Science* Express
DOI: 10.1126/science.1226344

This PDF file includes:

Correction: The dbGaP accession number on p. 5 has been corrected.

Materials and Methods

Phase II clinical trial of everolimus

Forty-five patients with progressive metastatic urothelial carcinoma were enrolled in an open-label, single-arm, non-randomized phase II study of the mTORC1 inhibitor everolimus (RAD001) from 02/2009-11/2010 (ClinicalTrials.gov number NCT00805129). Thirty-seven patients received everolimus for sufficient duration (dose of 10mg orally once daily) to be evaluable for the primary endpoint of 2-month progression-free survival. The median progression-free and overall survivals were 3.3 months (95% CI 2.7, 3.7) and 9.8 months (95% CI 7.8, 15.2), respectively. In addition to the index case studied here, one patient exhibited a partial response of 5.9 months in duration, while the remainder of the participants had stable disease or disease progression as best response. Based on the trial's pre-specified statistical design, everolimus was deemed inactive as a single agent and further development of everolimus in this disease was thus in doubt.

Sample preparation, sequencing, and analysis

Tumor tissue was collected after obtaining consent under an IRB-approved tissue acquisition protocol (89-076). DNA was extracted from tissue samples or blood using the Qiagen DNEasy Blood and Tissue Extraction Kit and Ficoll-Paque™. All samples were macro-dissected to ensure >70% tumor content. For the 96-tumor set, all exons of *TSC1* and *NF2* were sequenced using Sanger biochemistry.

The complete genomes of the tumor and matched normal samples were sequenced from 2x100bp libraries to ~40-fold haploid coverage using Illumina HiSeq instrumentation following manufacturer's protocols (Illumina, San Diego, CA) and aligned to build hg19 of the NCBI reference genome assembly using the CASAVA pipeline. Aligned reads were processed with Picard tools (Fennel T. *et al.*; http://picard.sourceforge.net/) and the Genome Analysis Toolkit pipeline (GATK) (*5, 6*). Duplicate reads in individual BAM files (*7*) were marked and removed. Multiple sequence realignment was performed for reads spanning candidate small insertions and deletions (indels) to correct likely misalignments, after which we performed base quality re-calibration (*5*). Somatic point mutations were detected with *MuTect* (March 2011 beta release), a Bayesian framework described elsewhere [refs (*8–11*) and https://confluence.broadinstitute.org/display/CGATools/MuTect]. A total of 2,758,394,298bp qualified as sufficiently covered for variant detection (89.1% of genome sequence), and from which mutation rates were determined. Indels were identified with the UnifiedGenotyper (GATK v1.0.5506) (*5*) from only bases called and reads aligned with a minimum quality score of 20. Somatic indels were those identified as variant in the tumor, genotyped as wild-type in the matched normal, and from a minimum read count identical to that of single-nucleotide variant detection (14 and 8 reads in the tumor and normal respectively). Only somatic and germline variants of >10% variant frequency were retained, excluding those present in 1000 genomes (*12*) or dbSNP130 not including the overlap with COSMIC release 47 (*13*). Indels were also excluded if they: (i) had excessive strand bias or were (ii) from regions of the genome with poor or zero mapping quality, or were (iii) those associated with a homopolymer run of >5bp. All remaining

somatic mutations were annotated for their sequence context and their effect on protein function was assessed computationally (*14*).

Structural rearrangements were detected with the Geometric Analysis of Structural Variants algorithm (GASV) (*15*). Candidate somatic rearrangements were retained if supported by >3 atypically paired reads in the tumor sample that was lacking from the matched normal genome after excluding clusters of reads where either pair aligned with a quality <132 (threshold derived from the shoulder of the empirical distribution of mapping qualities from the Illumina pipeline). Rearrangements were annotated (one or both breakpoints) for overlap with known sequence gaps, copy number variants (CNVs) in normal human populations, low-complexity/repeat structure, their intrinsic copy number (see below), their position in the footprint of protein-coding or non-coding genes genome-wide, and all were manually reviewed to exclude unfiltered alignment artifacts.

DNA copy number alterations (CNA) were determined from both whole-genome sequence data and Agilent array comparative genomic hybridization (aCGH) data. Copy number segmentation of sequence data was performed with seqCBS (with the exact Binomial likelihood statistic and default parameters) (*16*). For aCGH analysis, tumor DNA was co-hybridized with a pooled reference DNA to Agilent 1M aCGH arrays according to the manufacturer's instructions (Agilent Technologies, Wilmington, DE). Raw data were normalized and probe-level data were segmented with Circular Binary Segmentation and analyzed with RAE, all as previously described (*11, 17–19*).

Targeted exon sequencing

All protein-coding exons of 204 genes were sequenced in DNAs extracted from five frozen *TSC1*-mutant bladder tumors and genetically matched normal FFPE bladder tissue. In total, 250ng of DNA per sample were sheared for 300 seconds (Covaris; duty cycle = 10%, intensity = 5, cycles/burst = 200), and barcoded libraries were prepared using the TruSeq DNA Prep Kit (Illumina). An equimolar pool of the barcoded libraries was created and 1200ng was input to exon capture using the SureSelect Target Enrichment Kit (Agilent) with custom probes designed to target the coding exons of 204 genes. Capture by hybridization was performed according to the manufacturer's protocols with two exceptions: (A) we added to the hybridization reaction 600 picomoles of a pool of blocker oligonucleotides designed to be complementary to the barcoded Illumina adapters, and (B) we used PCR primers corresponding to the common flanking sequence of the Illumina adapters for the post-capture PCR reaction. The pooled capture library was quantified by Qubit (Invitrogen) and Bioanalyzer (Agilent) and sequenced in an Illumina HiSeq 2000 as 2x75bp reads. The resulting mean non-duplicate on-target coverage was 368-fold. Somatic mutations and indels were called using MuTect and GATK (described above). Variants observed in multiple distinct reads were considered to be somatic if they occurred in <1% of all sequence reads within matching normal tissue.

To validate the utility of the exon capture and deep sequencing method using FFPE derived DNA, we compared the results obtained using matched frozen and FFPE material from 6 patients, all with TSC1-mutant tumors (**Figs. S1B and C**). We observed 97% concordance among mutation calls in tumors where both matched frozen

and FFPE material were sequenced. The discordant 3% of mutation calls were present in the frozen tumors but at a lower allele frequency, likely indicative of intratumoral heterogeneity. We found no evidence that FFPE tumors produced an excess of false positive mutations by this approach.

Using an expanded 230 gene version of the exon capture and sequencing assay, we then analyzed 14 patients on the everolimus study with DNA extracted from FFPE-based bladder tumor tissue. Barcoded libraries were prepared as above and captured in two pools (mean non-duplicate on-target coverage was 326-fold). Variants present in the 1000 genomes project or dbSNP130 excluding overlap with the COSMIC database were filtered out as likely germline. Novel sequence variants in *TSC1* were validated and confirmed to be somatic by Sanger sequencing of tumor and normal DNA.

NF2 knockdown in TSC1-null bladder cancer cells

We hypothesized that inactivation of NF2, while rare in bladder cancers, may act in concert with TSC1 loss to further potentiate this patient's mTORC1 dependence. Indeed, prior studies have shown that NF2 loss enhances mTORC1 signaling and rapamycin sensitivity, through a PI3K-independent mechanism (*20*). We therefore performed short hairpin RNA (shRNA)-mediated knockdown of NF2 in the TSC1-null human bladder cancer cell line RT-4 (a generous gift from M. Knowles, Cancer Research UK Clinical Centre, Leeds, United Kingdom) using either pLKO.1 plasmids (clone TRCN0000039977) encoding shRNAs targeting NF2/merlin (Open Biosystems) or control shRNAs encoding a scrambled sequence (SHC002, Sigma-Aldrich). 293FT cells (Invitrogen) were transfected with the shRNA constructs as previously described (*2*) to generate viral supernatants followed by infection of TSC1-null RT-4 cells. Following puromycin selection, stably infected RT-4 cells were lysed and subjected to immunoblot analysis as previously described (*21*). Potent knockdown of NF2 expression with shRNA, but not scrambled control, resulted in enhanced sensitivity to the mTORC1 inhibitor rapamycin (see **Figs. S1D and E**).

Supplementary Text

Full Affiliations of the Authors:
Gopa Iyer[1,2,9], Aphrothiti J. Hanrahan[1], Matthew I. Milowsky[2,9], Hikmat Al-Ahmadie[3], Sasinya N. Scott[1], Manickam Janakiraman[1], Mono Pirun[5], Chris Sander[5], Nicholas D. Socci[6], Irina Ostrovnaya[7], Agnes Viale[8], Adriana Heguy[1], Luke Peng[1], Timothy A. Chan[1], Bernard Bochner[4], Dean F. Bajorin[2,9], Michael F. Berger[3], Barry S. Taylor[5,†,*], David B. Solit[1,2,9*]

[1]Human Oncology and Pathogenesis Program, Memorial Sloan-Kettering Cancer Center, New York, NY 10065
[2]Department of Medicine, Memorial Sloan-Kettering Cancer Center, New York, NY 10065
[3]Department of Pathology, Memorial Sloan-Kettering Cancer Center, New York, NY 10065

[4]Department of Surgery, Memorial Sloan-Kettering Cancer Center, New York, NY 10065
[5]Computational Biology, Memorial Sloan-Kettering Cancer Center, New York, NY 10065
[6]Bioinformatics Core Laboratory, Memorial Sloan-Kettering Cancer Center, New York, NY 10065
[7]Department of Biostatistics, Memorial Sloan-Kettering Cancer Center, New York, NY 10065
[8]Genomics Core Laboratory, Memorial Sloan-Kettering Cancer Center, New York, NY 10065
[9]Department of Medicine, Weill Medical College of Cornell University, New York, NY 10065

*Correspondence to: barry.taylor@ucsf.edu, solitd@mskcc.org
†Present address: Departments of Epidemiology and Biostatistics, Medicine, and the Helen Diller Family Comprehensive Cancer Center, University of California, San Francisco.

Acknowledgments: The authors would like to acknowledge C. Sawyers for critical reading of the manuscript, and G. Getz and K. Cibulskis for sharing a pre-publication version of the MuTect algorithm. This work was supported in part by the Michael and Zena Wiener for Therapeutics Program in Bladder Cancer; a Stand Up to Cancer Dream Team Translational Research Grant, a Program of the Entertainment Industry Foundation (D.B.S.); Mr. William H. Goodwin and Mrs. Alice Goodwin and the Commonwealth Foundation for Cancer Research, the Experimental Therapeutics Center of Memorial Sloan-Kettering Cancer Center; the Geoffrey Beene Cancer Research Center at Memorial Sloan-Kettering Cancer Center; an American Society of Clinical Oncology Young Investigator Award (G.I.) and the David H. Koch Foundation (B.S.T.). Funding for the phase II clinical trial of everolimus in advanced urothelial cancer was provided by Novartis Pharmaceuticals. The compressed binary Sequence Alignment/Map files (BAM) have been deposited in dbGaP under accession no. phs000535.v1.p1.

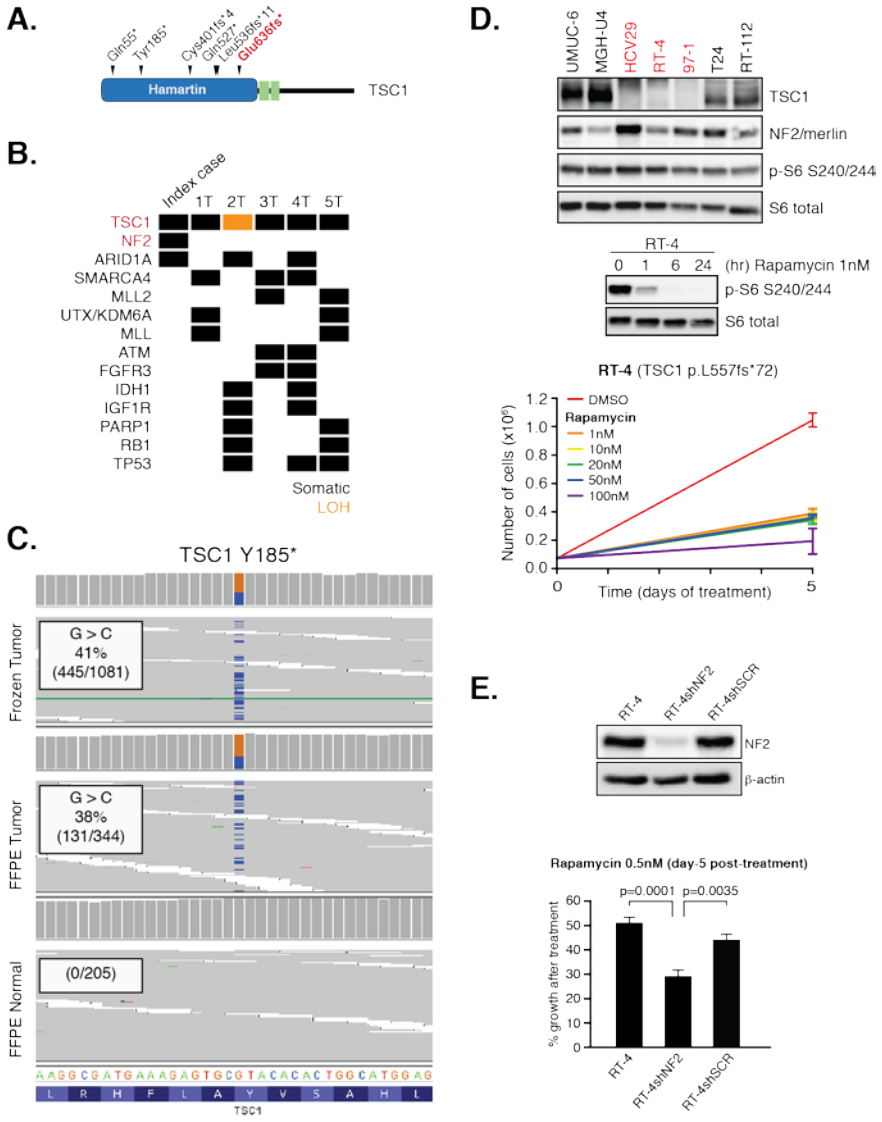

Fig. S1.

TSC1 mutations identified in the primary tumor of the index patient (red) and the 96-tumor validation cohort (black); domain structures are as indicated. **B.** The screening of five bladder tumors harboring TSC1 mutations using the exon capture assay identified a complex pattern of co-mutated genes. Genes mutated in two or more cases are shown. **C.** A somatic mutation in TSC1 (Y185*) was detected at comparable variant frequencies with high coverage in both frozen and FFPE tumors from the exon capture assay. **D.** Expression profile by immunoblotting (*top*) of TSC1, NF2, phospho-S6 Ser240/244, and total S6 in a panel of bladder cancer cell lines (red: TSC1-mutant cell lines). Beneath are immunoblots of p-S6 Ser240/244 and total S6 from whole cell lysates of TSC1-null RT-4 cells following treatment with 1nM rapamycin for 0 to 24 hrs. At bottom, the difference in cell count (RT-4) after 5 days of rapamycin at increasing concentrations is compared to control (DMSO). **E.** NF2/merlin knockdown following infection with short-hairpin lentiviral vectors (*top*) targeting NF2 (shNF2) or scrambled control (shSCR) in TSC1-null RT-4 cells. Growth is quantified after treatment with DMSO or 0.5nM rapamycin for

5 days (*bottom*; mean ± S.E. of n≥4 experiments; p-values: unpaired two-tailed Student's t-test). This experiment was repeated with a second shRNA targeting NF2 with comparable results (data not shown).

References and Notes

1. Materials and methods are available as supplementary materials on *Science* Online.

2. M. A. López-Lago, T. Okada, M. M. Murillo, N. Socci, F. G. Giancotti, Loss of the tumor suppressor gene NF2, encoding merlin, constitutively activates integrin-dependent mTORC1 signaling. *Mol. Cell. Biol.* **29**, 4235 (2009). doi:10.1128/MCB.01578-08 Medline

3. F. M. Platt *et al*., Spectrum of phosphatidylinositol 3-kinase pathway gene alterations in bladder cancer. *Clin. Cancer Res.* **15**, 6008 (2009). doi:10.1158/1078-0432.CCR-09-0898 Medline

4. D. A. Krueger *et al*., Everolimus for subependymal giant-cell astrocytomas in tuberous sclerosis. *N. Engl. J. Med.* **363**, 1801 (2010). doi:10.1056/NEJMoa1001671 Medline

5. M. A. DePristo *et al*., A framework for variation discovery and genotyping using next-generation DNA sequencing data. *Nat. Genet.* **43**, 491 (2011). doi:10.1038/ng.806 Medline

6. A. McKenna *et al*., The Genome Analysis Toolkit: a MapReduce framework for analyzing next-generation DNA sequencing data. *Genome Res.* **20**, 1297 (2010). doi:10.1101/gr.107524.110 Medline

7. H. Li *et al*.; 1000 Genome Project Data Processing Subgroup, The Sequence Alignment/Map format and SAMtools. *Bioinformatics* **25**, 2078 (2009). doi:10.1093/bioinformatics/btp352 Medline

8. M. F. Berger *et al*., The genomic complexity of primary human prostate cancer. *Nature* **470**, 214 (2011). doi:10.1038/nature09744 Medline

9. M. A. Chapman *et al*., Initial genome sequencing and analysis of multiple myeloma. *Nature* **471**, 467 (2011). doi:10.1038/nature09837 Medline

10. N. Stransky *et al*., The mutational landscape of head and neck squamous cell carcinoma. *Science* **333**, 1157 (2011). doi:10.1126/science.1208130 Medline

11. D. Bell *et al*.; Cancer Genome Atlas Research Network, Integrated genomic analyses of ovarian carcinoma. *Nature* **474**, 609 (2011). doi:10.1038/nature10166 Medline

12. R. M. Durbin *et al*.; 1000 Genomes Project Consortium, A map of human genome variation from population-scale sequencing. *Nature* **467**, 1061 (2010). doi:10.1038/nature09534 Medline

13. S. A. Forbes *et al*., The Catalogue of Somatic Mutations in Cancer (COSMIC), *Curr Protoc Hum Genet* Chapter 10, Unit 10 11 (2008).

14. B. Reva, Y. Antipin, C. Sander, Predicting the functional impact of protein mutations: application to cancer genomics. *Nucleic Acids Res.* **39**, e118 (2011). doi:10.1093/nar/gkr407 Medline

15. S. Sindi, E. Helman, A. Bashir, B. J. Raphael, A geometric approach for classification and comparison of structural variants. *Bioinformatics* **25**, i222 (2009). doi:10.1093/bioinformatics/btp208 Medline

16. J. J. Shen, N. R. Zhang, Change-point model on non-homogeneous poisson processes with applications in copy number profiling by next-generation DNA sequencing. *Preprint, Technical Report 257* Division of Biostatistics, Stanford University, http://statistics.stanford.edu/~ckirby/techreports/BIO/BIO 257.pdf (2011).

17. R. McLendon *et al*.; Cancer Genome Atlas Research Network, Comprehensive genomic characterization defines human glioblastoma genes and core pathways. *Nature* **455**, 1061 (2008). doi:10.1038/nature07385 Medline

18. B. S. Taylor *et al*., Functional copy-number alterations in cancer. *PLoS ONE* **3**, e3179 (2008). doi:10.1371/journal.pone.0003179 Medline

19. E. S. Venkatraman, A. B. Olshen, A faster circular binary segmentation algorithm for the analysis of array CGH data. *Bioinformatics* **23**, 657 (2007). doi:10.1093/bioinformatics/btl646 Medline

20. M. F. James *et al*., NF2/merlin is a novel negative regulator of mTOR complex 1, and activation of mTORC1 is associated with meningioma and schwannoma growth. *Mol. Cell. Biol.* **29**, 4250 (2009). doi:10.1128/MCB.01581-08 Medline

21. C. A. Pratilas *et al*., Genetic predictors of MEK dependence in non-small cell lung cancer. *Cancer Res.* **68**, 9375 (2008). doi:10.1158/0008-5472.CAN-08-2223 Medline